Fibre Science and Technology 13 (1980) 385-395

STRESS WAVE PROPAGATION IN FIBRES: EFFECT OF CROSSOVERS

DAVID ROYLANCE

Department of Materials Science and Engineering,
Massachusetts Institute of Technology, Cambridge, Massachusetts 02139 (USA)

SUMMARY

A direct numerical solution is described which models the wave propagation dynamics of a system of two crossed fibres, one of which has been subjected to transverse ballistic impact. The model provides a means of assessing the influence of fibre materials properties and fibre–fibre slip on the complex wave phenomena occurring at fibre crossovers. This is a matter of considerable importance in rationalising the performance of textile structures used as ballistic protection devices.

INTRODUCTION

This paper reports on a numerical study of the dynamics of a special but highly important physical system: that of two fibres, one having been transversely impacted at zero obliquity by a high-speed projectile, and the other crossing the first perpendicularly at some distance from the impact point. This system is germane to the understanding of impact and wave propagation phenomena in woven textile panels used for ballistic protection of personnel and equipment. Wave propagation phenomena occurring at fibre crossovers have a very strong influence on the ballistic response of a panel, since a typical woven panel has of the order of a million crossovers per square meter, each of which effects the intensity of stress waves propagating away from the impact point. Some fibre–fibre slippage is often noted in post-mortem examinations of impacted fabrics, and one would expect that the extent of slippage might also affect the nature of the fabric transient response.

Although the initial response of a single fibre to high-speed transverse impact is describable by closed-form algebraic expressions,[1] the late-time effects associated with wave reflections from fibre crossovers and subsequent interactions between reflected and ongoing waves are intractable by closed-form methods. One seeks a

Fibre Science and Technology 0015-0568/80/0013-0385/$02·25
Printed in Great Britain

numerical approach which can take due advantage of the effectively one-dimensional nature of fibres. Such a numerical approach was developed by Davids,[2] who used an explicit finite-difference method based on a discrete formulation of the governing dynamic equations. This method has been found to be well suited to the analyses of fibres[3,4] and fabrics,[5] and its use in the present crossed-fibre system will be detailed below.

METHOD OF SOLUTION

System idealisation

The system of two crossed fibres is modelled as in Fig. 1, where the origin of coordinates is placed at the midpoint of the clamped primary fibre, which extends along the x-axis. The projectile moves along the y-axis only, and impacts the primary fibre at the origin. From symmetry, only half the primary fibre need be considered. The secondary fibre extends along the z-axis and intersects the primary fibre at some arbitrary distance from the origin. At the crossover point, the secondary fibre is assumed to follow the motion of the primary fibre in the direction perpendicular to the primary fibre (in the x–y plane), but is allowed some measure of slip in the direction parallel to the primary fibre. Motion of the primary fibre is assumed to occur in the x–y plane only, while the secondary fibre may move in all three directions.

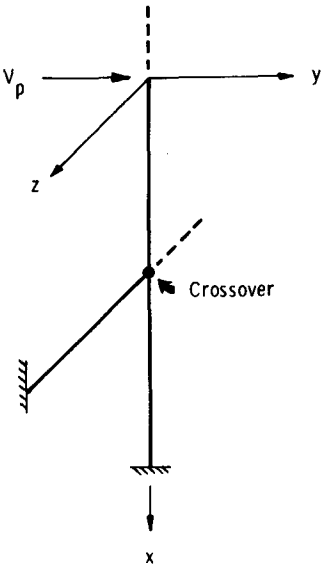

Fig. 1. Schematic of model for numerical analysis of two crossed fibres.

To proceed, the fibres are discretised as a series of n pin-jointed finite elements of equal length as shown in Fig. 2. The masses of the elements are taken to be lumped at the nodal end points of these elements, and at these nodes are defined vector coordinates $\mathbf{x}_i$, velocity $\mathbf{v}_i$, and tension $\mathbf{T}_i$. The scalar strain ε_i at each element will be computed from the coordinates of the nodes at either end of the element. The tension $\mathbf{T}_i$ has the same direction as the element itself (approximating the element's assumed inability to support a bending moment), while $\mathbf{v}_i$ is not constrained in direction. These elements are now described by simple governing equations: impulse–momentum balance, strain–displacement relation, constitutive relation, etc. These relations are cast as a recursive algorithm for proceeding from one element to the next along the fibre length, and then repeating the process at a new increment of time. The computer solution is referenced to a Lagrangian frame of reference attached to and extending with the fibre, which effectively reduces the problem to one dimension.

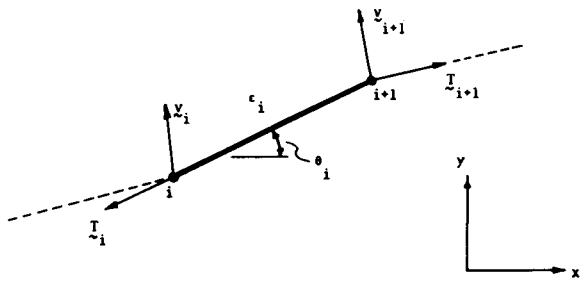

Fig. 2. Discrete element of fibre.

Momentum balance

A consideration of impulse–momentum balance at the $i+1$st node provides a means of computing the current velocity at that node in terms of its velocity at the beginning of the previous time increment and the tensions acting on it during that time increment. (In the following, subscripts on a variable refer to the node at which it is defined, while superscripts t and $t-1$ refer to values at the current and previous times respectively.) The impulse–momentum balance can be written in finite difference form as:

$$\mathbf{T}_{i+1}^{t-1} - \mathbf{T}_i^{t-1} = \frac{\Delta m}{\Delta t}(\mathbf{v}_{i+1}^t - \mathbf{v}_{i+1}^{t-1}) \tag{1}$$

Letting $A = \Delta t/\Delta m$, a fixed parameter, eqn (1) may be solved for $\mathbf{v}_{i+1}^t$:

$$\mathbf{v}_{i+1}^t = \mathbf{v}_{i+1}^{t-1} + A(\mathbf{T}_{i+1}^{t-1} - \mathbf{T}_i^{t-1}) \tag{2}$$

The boundary conditions are easily incorporated into the impulse–momentum balance: at the first node, the velocity is set equal to the current projectile velocity ($\mathbf{v}_1^t = \mathbf{v}_p^t$), and at the clamp the velocity is set to zero ($\mathbf{v}_n^t = 0$).

Strain–displacement relation

Having computed the velocities at the ith and $i+1$st nodes the strain in the element between these nodes is computed as:

$$\Delta\varepsilon_i = (L_i^t - L_i^{t-1})/L_i^t) \tag{3}$$

where L_i is the scalar element length. Continuing:

$$\varepsilon_i^t = \varepsilon_i^{t-1} + (L_i^t/L_i^{t-1}) - 1 \tag{4}$$

where

$$L_i^{t-1} = |\mathbf{x}_{i+1}^{t-1} - \mathbf{x}_i^{t-1}| \tag{5}$$

and

$$L_i^t = |\mathbf{x}_{i+1}^t - \mathbf{x}_i^t| = |(\mathbf{x}_{i+1}^{t-1} + \mathbf{v}_{i+1}^t \Delta t) - (\mathbf{x}_i^{t-1} + \mathbf{v}_i^t \Delta t)| \tag{6}$$

Constitutive relation

Knowing the strain ε_i^t, the tension magnitude T_i^t is computed from the material's dynamic stress–strain law. The numerical results reported in this paper will be restricted to linear elastic materials, for which the tension is computed as:

$$T_i^t = E\varepsilon_i^t \tag{7}$$

where E is the Young's modulus. Other constitutive models could also be used without difficulty, and the code as presently developed contains routines for nonlinear elasticity (polynomial or exponential strain hardening), and for both linear and nonlinear viscoelasticity. The reader is referred elsewhere[6] for a more detailed account of the use of these other models in the analysis of fibre and fabric impact.

Computation of new projectile velocity

The algorithm described above proceeds from one element to the next along the length of fibre, and is started by imposing the initial projectile velocity on the first node. At the end of the first time increment, a strain will have developed in the first element due to the velocity difference between the first and second nodes. (Initially, all velocities, tensions, and strains are set to zero.) This strain produces a tension as calculated from the constitutive relation, and this tension produces a velocity in the second node beginning at the next time increment.

After each time increment, at the completion of the lengthwise recursive calculations, a new projectile velocity v_p^t can be computed by means of a momentum balance using the tension at the first node:

$$-2T_y = m_p \frac{\Delta v_p}{\Delta t} = m_p \frac{v_p^t - v_p^{t-1}}{t} \tag{8}$$

where m_p is the projectile mass, T_y is the component of fibre tension in the projectile

travel direction, and the factor 2 accounts for the other half of the primary fibre extending in the $-x$ direction.

Crossover fibre calculations

Computation of field variables along the secondary fibre proceeds in a lengthwise manner exactly as described above, although the vector resolutions become slightly more complicated due to the motion in three rather than two dimensions. The secondary algorithm is started by imposing on the first node of the crossover fibre the velocity imparted to it by the primary fibre. As stated earlier, the secondary fibre is allowed a measure of slip along the primary fibre but is constrained to follow it in the direction normal to the primary fibre. Denoting the node on the primary fibre nearest the crossover point as ix, the velocity of this node resolved in directions parallel and perpendicular to the primary fibre there are:

$$v^t_{\text{para}} = u^t_{ix} \cos \theta^t_{ix} + v^t_{ix} \sin \theta^t_{ix} \tag{9}$$

$$v^t_{\text{perp}} = v^t_{ix} \cos \theta^t_{ix} - u^t_{ix} \sin \theta^t_{ix} \tag{10}$$

$$\theta^t_{ix} = \tan^{-1} [(y1^t_{ix} - y1^t_{ix-1})/(x1^t_{ix} - x1^t_{ix-1})] \tag{11}$$

In eqn (11), notation of the form $y1$ or $y2$ indicates field variables for the primary and secondary fibres respectively. The velocity imposed on the first (crossover) node of the secondary fibre is:

$$u2^t_1 = \alpha_s v^t_{\text{para}} \cos \theta^t_{ix} - v^t_{\text{perp}} \sin \theta^t_{ix} \tag{12}$$

$$v2^t_1 = \alpha_s v^t_{\text{para}} \sin \theta^t_{ix} + v^t_{\text{perp}} \cos \theta^t_{ix} \tag{13}$$

$$w2^t_1 = 0 \tag{14}$$

where α_s is a slide factor which permits no sliding when set to 1 and unrestrained sliding when set to zero.

The crossover node ix will change with time if the tangential slip along the primary fibre is sufficient. After each time increment, a new position of the first node on the secondary node is computed, and ix is assigned to the nearest node on the primary fibre.

The momentum–balance calculation of $\mathbf{v}^t_{i+1}$ in the primary fibre must be modified when the $i + 1$st node is also the crossover node ix, since the secondary fibre applies its own tension to that node. Denote the direction angles of the primary and secondary fibres at that node as $\phi 1_x$, $\phi 1_y$, $\phi 1_z$ and $\phi 2_x$, $\phi 2_y$, $\phi 2_z$ respectively ($\phi 1_z = 0$). Then the components of tension applied by the secondary fibre, resolved along directions parallel and perpendicular to the primary fibre are:

$$T2^t_{\text{para}} = T2^t_1 [\cos \phi 2_x \cos \phi 1_x + \cos \phi 2_y \cos \phi 1_y] \tag{15}$$

$$T2^t_{\text{perp}} = T2^t_1 [\cos \phi 2_y \cos \phi 1_x - \cos \phi 2_x \cos \phi 1_y] \tag{16}$$

where the direction cosines are computed from the current nodal coordinates. The primary fibre is allowed to feel the impulse of the perpendicular component fully,

but the parallel component is reduced by the slide variable α_s. The usual computation of $\mathbf{v}^t_{i+1}$ is then adjusted as:

$$ul^t_{i+1} \leftarrow ul^t_{i+1} + 2A[T2^t_{\text{perp}} \cos\phi 1_y + \alpha_s T2^t_{\text{para}} \cos\phi 1_x] \tag{17}$$

$$vl^t_{i+1} \leftarrow v^t_{i+1} + 2A[T2^t_{\text{perp}} \cos\phi 1_x + \alpha_s T2^t_{\text{para}} \cos\phi 1_y] \tag{18}$$

where the $\leftarrow$ symbol indicates a computer replacement operation; i.e. the additional impulse from the secondary fibre is added to that already computed from eqn (2).

Stability, accuracy and efficiency

Criteria for stability and accuracy of the above method are related to the theory of characteristics for hyperbolic systems of partial differential equations and are similar to those for finite-difference solutions of wave propagation problems.[7] Given a wave equation of the form

$$\partial^2 u/\partial t^2 = c^2(\partial^2 u/\partial x^2) \tag{19}$$

which is to be solved by approximating ∂t and ∂x by finite differences Δt and Δx, a stability ratio α can be defined as

$$\alpha = c(\Delta t/\Delta x) \tag{20}$$

The finite-difference scheme is stable and accurate for $\alpha = 1$, stable but increasingly inaccurate for $\alpha < 1$, and unstable for $\alpha > 1$. The choices for Δx and Δt are thus not independent, but are related by the wavespeed for the choice of $\alpha = 1$.

In the direct analysis of the fibres described above, this stability criterion is equivalent to adjusting the rate of march of the computer solution along the fibre to match the rate of propagation of the strain wave. Conceptually, this requirement is related to the necessity of programming the finite governing equations so as to model the actual continuous dynamic process as accurately as possible. If a major disturbance—such as the passage of a strain wave with its accompanying energy input—takes place in a finite element which is not considered explicitly in the computational scheme, divergent numerical results are very likely.

Once a stable computational scheme has been developed, one usually attempts to increase its accuracy to whatever limit is desired by decreasing the size of the elements, i.e. by increasing the number of nodes. Since for $\alpha = 1$ a decrease in Δx requires a corresponding decrease in Δt, the computation time—and therefore the expense—required for analysis of a given impact event increases as the square of the number of nodes. The element size is therefore chosen so as to balance the conflicting requirements of economy and accuracy. As an example of computation time, the CPU requirement for the IBM 370/168 system was 10·1 s for a problem in which the strain wave propagated 0·2 m along the primary fibre and 0·1 m along the secondary fibre, with a length increment of 2·0 mm. As a means of improving code efficiency, the program employs logical flags which terminate the length loop computation when the computer passes the point along the fibre length corresponding to the wavefront.

Accuracy assessment for the case of two crossed fibres is difficult, since no experimental or closed-form mathematical analysis of this problem is available. However, some assurance of accuracy was derived by performing computer experiments in which both the primary and secondary fibres were placed at the origin (the impact point). In this case, both of the fibres responded as in single-fibre impact, and these results could be compared with earlier studies.[4] These results agreed identically. Checking of the crossover interactions was performed manually, but no other verification procedures were attempted.

As with most discrete–variable solutions, problems were encountered with overshoot and numerical oscillation at regions of discontinuity near the wavefront and the crossover point. These oscillations could be diminished by incorporating artificial viscosity into the material constitutive model, but the results to be presented below were obtained without such smoothing.

RESULTS AND DISCUSSION

Figure 3 shows typical results obtained from the above described computer treatment, in this case for two crossed aramid fibres (modulus = 58·6 GPa), the crossover point being 10 cm along the primary fibre from the impact point. The fibres were assumed to respond elastically, and no sliding was permitted at the crossover ($\alpha_s = 1$). The figure shows the distribution of strain in each fibre 28·7 μs after impact at 400 m/s, where the abscissa measures the distance along the primary fibre from the origin and along the secondary fibre from the crossover point. The dotted line at strain = 1·45 % depicts the level of strain which would be generated in a single fibre at this impact velocity. In this example no artificial viscosity has been

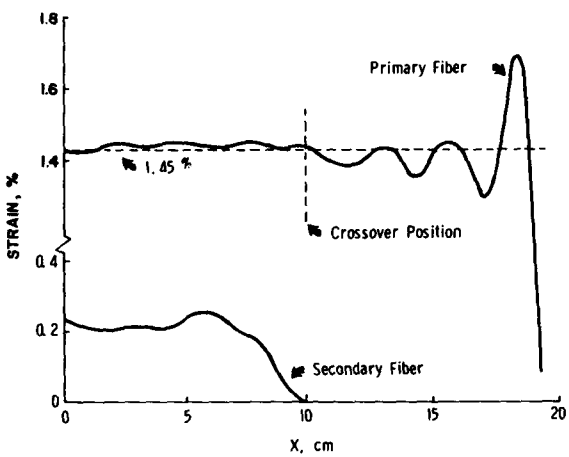

Fig. 3. Strain distributions in two crossed aramid fibres, 28·7 μs after impact at 400 m/s.

included, and the large overshoot at the wavefront causes problems in interpretation of results. In spite of this oscillatory behaviour, however, an increase in strain in the primary fibre behind the crossover due to the wavelet reflected from the crossover is evident, as is a reduction in the strain intensity in the region of the primary fibre beyond the crossover. More easily measured is the level of strain intensity diverted to propagate along the secondary fibre.

Computer experiments were conducted on the crossover system for a range of fibre moduli and slide factors, and graphical output similar to Fig. 3 used to determine coefficients of wave reflection, transmittance and diversion. These coefficients are defined as that fraction of the outward-propagating strain wave which is reflected backwards by the crossover, the fraction which passes through the crossover and continues its outward propagation, and the fraction which is diverted and begins propagating along the fibre passing transversely through the crossover. As a means of obtaining these coefficients in spite of the uncertainties caused by the numerical fluctuations near the wavefronts, the computer was asked to determine the average strain level over a portion of the fibre length away from the oscillation region. In order to guarantee conservation of energy, the sum of the squares of the above three coefficients should equal unity; this was in fact obtained and offers some assurance as to the accuracy of the numerical values.

The variation in the transmission and diversion coefficients with fibre modulus is shown in Fig. 4. The coefficients of reflection were near 1% over this range of moduli, but showed considerable scatter. It is seen that only the diversion coefficient is of a much larger magnitude than the reflection coefficient, and that it varies more

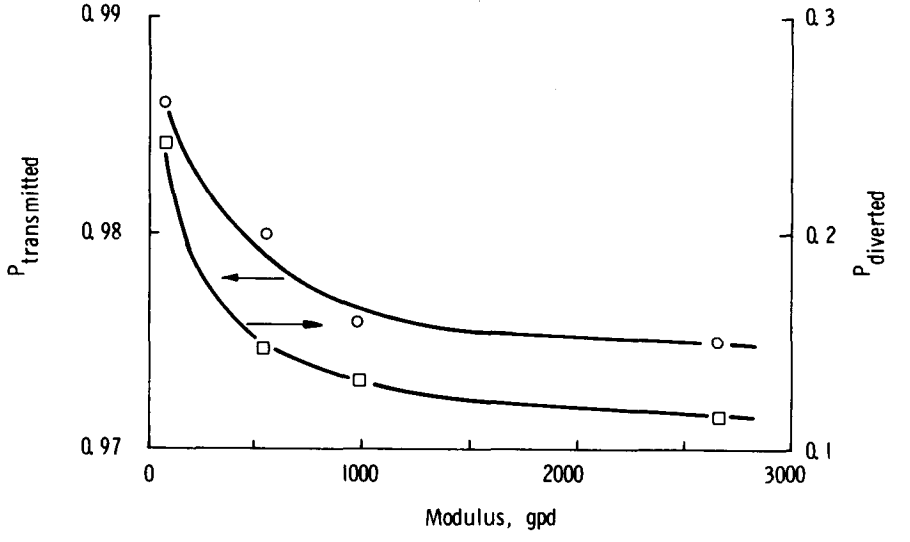

Fig. 4. Influence of fibre modulus on coefficients of wave transmission and diversion.

strongly with the fibre modulus. The major portion of the crossover influence on wave propagation is thus ascribed to diversion rather than reflection.

As the slide factor α_s decreases from unity toward zero, representing less fibre–fibre friction at crossover points, one would expect that the reflection and diversion coefficients would approach zero and that the transmission coefficient would approach unity. At $\alpha_s = 0$, there is no coupling between the two fibres (until the arrival of the transverse kink wave, which generally occurs later than the arrival of the longitudinal wave). As seen in Figs 5, 6 and 7 respectively for aramid fibres, this trend is quantified by the results of the crossover computations.

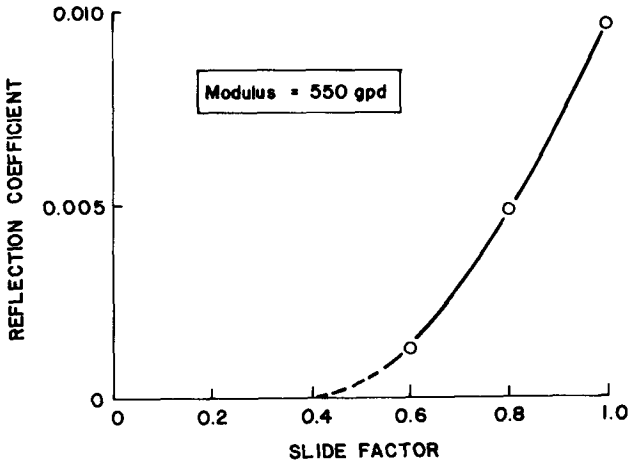

Fig. 5. Influence of fibre–fibre slippage on stress wave reflection.

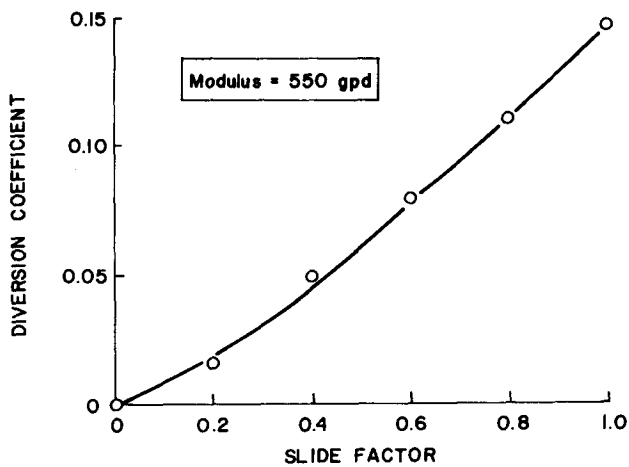

Fig. 6. Effect of slippage on wave diversion.

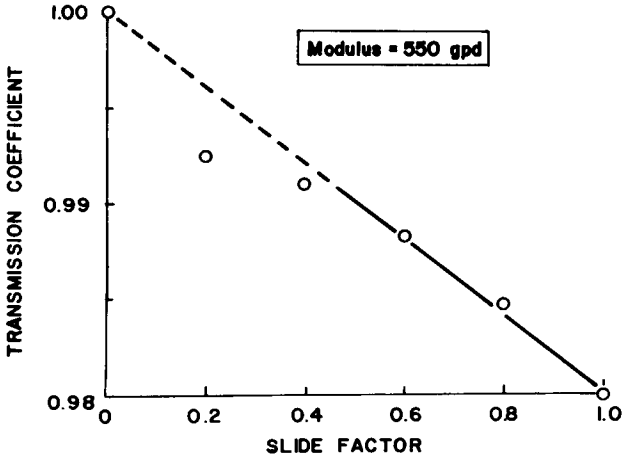

Fig. 7. Effect of slippage on wave transmission.

CONCLUSIONS

Although it was necessary to employ an averaging procedure to avoid misinterpretation due to numerical oscillation at wavefronts, the numerical model employed here was sufficient to determine the salient features of wave propagation at fibre crossovers: the influence of wave diversion is much stronger than that of reflection, the extent of wave diversion decreases with fibre modulus, and the influence of the crossover diminishes as the extent of sliding increases. These observations are of value in improving one's intuition as to the effect of crossovers during ballistic impact on a woven panel, but beyond this they may also be incorporated explicitly in numerical analyses of panel impact. Some computer experiments have been performed in which wave reflection–diversion models are compared with direct finite-difference analyses of panel impact, and the conclusions of these comparisons will be the subject of a later paper.

ACKNOWLEDGEMENTS

This study was supported by the US Army Natick Research and Development Command under contract DAAG-76-C-1003, with Dr Roy Laible acting as technical monitor. Receipt of this support is gratefully acknowledged.

REFERENCES

1. J. C. SMITH, F. L. MCCRACKIN and H. F. SHIEFER, Stress–strain relationships in yarns subjected to rapid impact loading. Part V: Wave propagation in long textile yarns impacted transversely, *Textile Res. J.*, **28** (1958) pp. 288–302.

2. M. L. WENNER, 'Viscoelastic waves with reflection for longitudinal impact' in *Stress Waves and Penetration*, (Ed. N. Davids), Final Report, The Pennsylvania State University, May 15, 1966.
3. F. DE S. LYNCH, 'Dynamic Response of Constrained Fibrous Systems Subjected to Transverse Impact. Part II: A Mechanical Model', Technical Report AMMRC TR70-16, Army Materials and Mechanics Research Center, Watertown, Massachusetts, July 1970.
4. D. K. ROYLANCE, Wave propagation in a viscoelastic fiber subjected to transverse impact, *J. Appl. Mech.*, **90**, pp. 143–8.
5. D. K. ROYLANCE, A. WILDE and G. TOCCI, Ballistic impact of textile structures, *Textile Res. J.*, **43** (1973) pp. 34–41.
6. D. K. ROYLANCE and S. S. WANG, Penetration mechanics of textile structures: Influence of non-linear viscoelastic relaxation, *Polym. Eng. and Sci.*, **18** (1978) pp. 1068–72.
7. S. H. CRANDALL, *Engineering Analysis*, McGraw-Hill, 1956 pp. 396–8.